20th Australasian Fluid Mechanics Conference
Perth, Australia
5-8 December 2016

Wake Symmetry Properties of Flexible Pitching Airfoils

E. Akoz[1], **S. Zeyghami**[1] **and K. W. Moored**[1]

[1]Mechanical Engineering & Mechanics
Lehigh University, Bethlehem, PA 18015, USA

Abstract

The wake structure and the performance of flapping airfoils are tightly connected to the kinematics and the flexibility of the airfoils. For rigid airfoils, Strouhal number (St), which is linked to the arrangements of the vortices in the wake, characterizes the influence of the kinematics. At large St vortex street behind the airfoil shifts from a symmetric to an asymmetric(deflected) configuration. In this study, we aim to investigate how flexibility of the foil influences wake deflection across a range of St by employing a two-dimensional boundary element fluid solver which is strongly coupled to a torsional spring structural model. It is found that the jet deflection dependence on Strouhal number vanishes for flexible systems. A dipole model better explains the symmetry-asymmetry characteristics of the wake. Together with the dipole model, the amount of phase delay in the first flapping cycle turns out to be the critical parameter which determines the wake symmetry.

Introduction

Fishes control their flexible appendages either actively or passively to propel themselves. The flexibility of the appendages has a major impact on the performance characteristics. A vast number of studies are conducted to understand the effect of chordwise flexibility on the propulsors and the optimum kinematics to drive them [12]. Gains of both thrust generation and efficiency is observed with proper selection of kinematics and structural stiffnesses which eventually dictates the bending pattern over the propulsor [1, 11].

An important kinematic parameter of a flapping system is Strouhal number(St), which is defined as $St = fA/U$, where f is the flapping frequency of the propulsor, A is the amplitude of motion and U is the free stream velocity. The flow field dependence of oscillating airfoils on Strouhal number is first studied by Jones et. al. (1998) both numerically and experimentally. Gradually increasing Strouhal numbers from 0.29 to 0.6, they observed a drag producing Karman vortex street, thrust producing reverse Karman vortex street and a deflected reverse Karman vortex street, respectively, behind a plunging airfoil. Further experimental and computational studies suggested that the transition from a horizontal to deflected vortex street happens around $St \sim 0.4$. [2,3,4,5].

Strouhal number essentially determines the arrangements of vortices in oscillating systems. The connection of the vortex spacing and the deflected jet formation is first introduced by Emblemsvag et. al. (2002). They suggest that pitching at high frequencies increases the strength of shed vortices, as well as, decreases the spacing between them, hence forming dipoles. Instead of using a Strouhal number threshold, Godoy-Diana et. al. (2009) developed a vortex dipole model to obtain the symmetry characteristic of the wake. Model compares a dipole velocity(translation speed of the dipole) and the induced velocity of the rest of the vortex street on dipole to determine the stability of the vortex street. Recently, Zheng & Wei (2012) proposed a simpler condition involving two consecutive dipoles for symmetry breaking behavior. Wake symmetry is preserved if the induced velocity of two consecutive dipoles are identical; otherwise, symmetry breaking occurs.

Introducing flexibility to an oscillating system is observed to inhibit the wake asymmetry. Marais et. al. (2012), conducted experiments and compared a pitching rigid airfoil with a flexible one. It was found that the jet behind the flexible airfoil remained symmetric for sufficiently large flapping amplitudes and chord-based Strouhal numbers. They concluded that the interaction of the shed vortices with the flexible structure neutralizes the deflection of the propulsive jet. Recently, Zhu et. al (2014) computationally studied the effect of the flexibility on wake symmetry properties with a larger parameter space and reported that flexibility can either inhibit or trigger wake symmetry breaking depending on the change in the effective angle of attack and the change in the trailing-edge flapping velocity of the airfoil.

In light of the above observations, we conducted a computational study to compare the flow structures of rigid and flexible pitching airfoils. Flexibility of the airfoils is modeled with a torsional spring which is located at the leading edge. A range of pitching frequencies and flexibilities are investigated to characterize the wake deflection across a range of Strouhal numbers.

Analysis

Computational Model and Validation

To model a high Reynolds(Re) number fluid flow, the field is assumed inviscid, irrotational and incompressible around the airfoils. The boundary layer next to the solid boundaries is very thin at high Re flows and, to a very good approximation, viscous effects become negligible. If the fluid is considered to be incompressible and irrotational, the continuity equation reduces to the Laplace's equation, $\nabla^2\phi = 0$, where ϕ is the velocity potential in the fluid domain. Following Katz & Plotkin, the solution to Laplaces equation is found by distributing source and doublet singularities on the problem boundaries(S_B, S_W), as illustrated in Figure 1 [7]. The boundary conditions need to be satisfied are;(1) the velocity component normal to the body's surface must be zero(no-flux boundary condition), (2) the disturbance created by the flow should decay far from the body(far-field boundary condition). The elementary solutions of the doublet and source both automatically fulfill the far-field boundary condition. No-flux boundary condition requires constant velocity potential inside the boundaries. Therefore, a general solution to the Laplace's equation can be written for an arbitrary point(P) inside the surface S_B as;

$$\phi(P) = \frac{1}{4\pi}\iint_{S_B}[\sigma(\frac{1}{r}) - \mu\frac{\partial}{\partial n}(\frac{1}{r})]dS - \frac{1}{4\pi}\iint_{S_W}\mu\frac{\partial}{\partial n}(\frac{1}{r})dS + \phi_\infty \tag{1}$$

where σ and μ are the strengths of source and doublet elements on the boundaries, respectively. $\phi(P)$ is the velocity potential of an arbitrary point, P, within the boundaries S_B, ϕ_∞ is the velocity potential at infinity and r is the distance from the singularity to

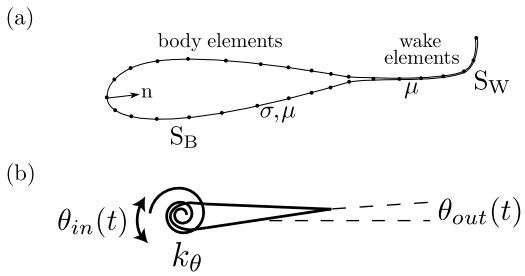

Figure 1: (a) The schematic of an airfoil whose body and wake domains(S_B, S_W) are discretized into elements. Each body element has a constant strength doublet (μ) and a source (σ) singularities whereas wake elements only have a constant strength doublet (μ) singularity. The normal vectors of each element is also shown as n. (b) The schematic of the torsional spring model with the spring constant k_θ, input pitching angle of θ_{in} and output passive pitching angle of θ_{out}

the point of interest (P location). Setting the internal velocity potential to the constant velocity potential at infinity, $\phi = \phi_\infty$, reduces the equation (1) to a simpler form:

$$\frac{1}{4\pi}\iint_{S_B}[\sigma(\frac{1}{r}) - \mu\frac{\partial}{\partial n}(\frac{1}{r})]dS - \frac{1}{4\pi}\iint_{S_W}\mu\frac{\partial}{\partial n}(\frac{1}{r})dS = 0 \qquad (2)$$

To solve the problem numerically, the geometry is divided into N panels, as shown in the Figure 1(a). The source strength is set to the prescribed value of $\sigma = \mathbf{n}\cdot Q_\infty$, where $\mathbf{n}$ is the normal vector on the surface pointing inwards and Q_∞ is the velocity far away from the body, and the integration is performed for each panel such that;

$$\sum_{j=1}^{N} C_j\mu_j + \sum_{k=1}^{N_w} C_k\mu_k - \sum_{j=1}^{N} B_j\sigma_j = 0 \qquad (3)$$

where

$$C_j = \frac{1}{4\pi}\int_{body}\frac{\partial}{\partial n}(\frac{1}{r})dS|_j \qquad (4)$$

$$C_k = \frac{1}{4\pi}\int_{wake}\frac{\partial}{\partial n}(\frac{1}{r})dS|_k \qquad (5)$$

$$B_j = -\frac{1}{4\pi}\int_{body}(\frac{1}{r})dS|_j \qquad (6)$$

N is the number of body panels and N_w is the number of wake panels.

This numerical scheme leads to N+1 unknowns(N body doublet strengths and the doublet strength of the first wake element) with N linear equations, one for each body panel element. To solve the linear system, explicit Kutta condition is forced in the trailing edge. The doublet strength of the first wake panel becomes; $\mu_w = -(\mu_1 - \mu_N)$ where $\mu_1 - \mu_N$ is the vortex strength at the trailing edge and μ_w is the doublet strength of the first wake panel.

At every time step, a panel element with a known doublet strength advects from the trailing edge with local velocity, rolls up and forms vortices in the wake region. During the roll up process, the ends of the wake doublet elements, which are point vortices, must be de-singularized for the numerical stability of the solution [8]. At a cutoff radius of $\varepsilon/c = 2.5\times10^{-4}$, the irrotational induced velocities from the point vortices are replaced

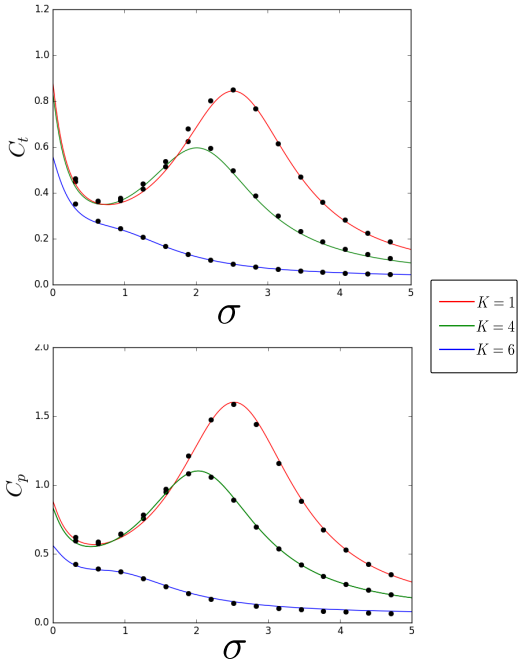

Figure 2: Coefficient of thrust and power as a function of reduced frequency. Solid lines are reproduced from Moore (2014) and show the analytical results for 3 different K values and black dots are our simulation results

with a rotational Rankine core model. The tangential perturbation velocity is found by local differentiation of the velocity potential. Then the pressure field acting on the body is calculated using unsteady Bernoulli equation.

A lumped flexibility model is used which consists of a torsional spring placed at the leading edge of the airfoil. The structure model is assumed ideal with no damping. The governing equations of the structure is therefore reduced to:

$$m\ddot{\theta} + k_\theta\dot{\theta} = M_{fluid} + M_{inertial} \qquad (7)$$

where M_{fluid} and $M_{inertial}$ are the moments due to the fluid pressure and inertial effects, respectively. m is the airfoil mass and k_θ is the spring stiffness constant. The governing equations of the solid are discretized using the trapezoidal rule, which is second order accurate in time, resulting in the following equation:

$$\begin{aligned}[k_\theta + (2/\delta t)^2 m]\theta_{n+1} = M_{fluid_{n+1}} + M_{inertial_{n+1}} \\ + m[(2/\delta t)^2\theta_n + (4/\delta t)\dot{\theta_n} + \ddot{\theta_n}]\end{aligned} \qquad (8)$$

Magnitude of the fluid and inertial moments at the present time step are not known. Thus, equation above is solved iteratively for θ_{n+1} until the convergence criteria is met; $\|{\theta_{n+1}}^{i+1} - {\theta_{n+1}}^{i}\| \leq \varepsilon$. Where ε is the tolerance and is set to 10^{-7}. An Aitken under relaxation method is used to improve the convergence rate.

The in-house solver is validated against an analytic model, so called torsional flexibility model, where a torsional spring is attached to the leading edge of a rigid airfoil. Moore (2014) obtained exact solutions for thrust and power by linearizing incompressible Euler equations using small amplitude motion assumption [10]. For the validation cases, we actively controlled the leading edge of the thin airfoil with a small amplitude heaving motion, as small as 0.1 % of the chord length($c = 0.1$m), and trailing edge followed with passive pitching. The results

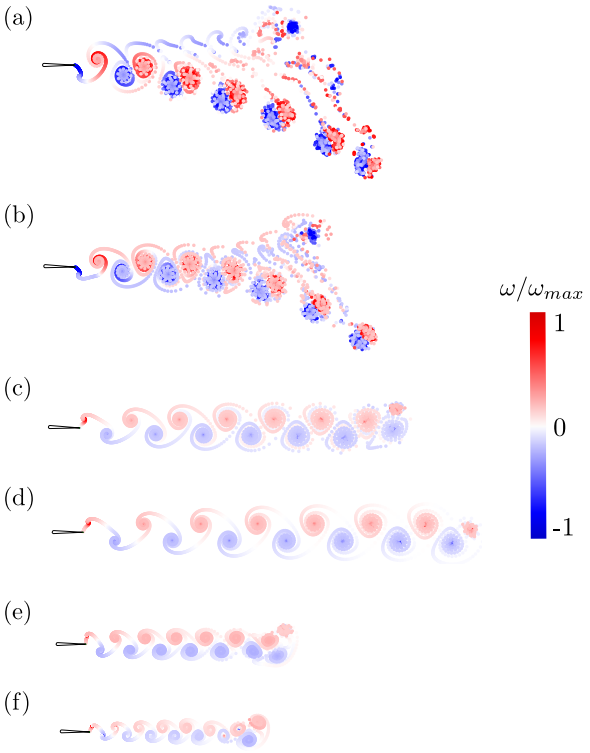

Figure 3: The comparison of a rigidly pitching airfoil(a), with airfoils of different non-dimensional flexibilities at $St \approx 0.5$, $\Pi = 0.1$ (b), $\Pi = 0.2$ (c), $\Pi = 0.3$ (d), $\Pi = 0.4$ (e),$\Pi = 0.5$ (f). The red and blue vortices represents the counter clockwise and clockwise vorticity, respectively.

are shown in Figure 2 for 3 different K values. K is a non-dimensional parameter, showing the ratio of spring stiffness to the fluid forces; $K = k_\theta/\rho U_\infty^2 c^2$, where ρ is the fluid density and U_∞ is the free-stream velocity. We observed a remarkable collapse of our simulation results with the analytical model, for both thrust and power coefficients as the non-dimensional driving frequency, $\sigma = \pi f c/U_\infty$, is varied.

Problem Formulation and Parameter Space

Computations are performed on two-dimensional 10% thick teardrop airfoils undergoing pitching motion. The flow structure of rigid airfoils are compared against flexible counterparts. Flexibility is modeled with a torsional spring in the leading edge as shown in Figure 1(b). Flexible airfoils are pitched actively from their leading edge and the trailing edge passively deflects in response to the forces acting on it. A non-dimensional flexibility Π, the ratio of fluid forces to the spring forces, is defined as $\Pi = \sqrt{\rho f^2 c^4/k_\theta}$. A rigid airfoil and 5 different flexible airfoils with Π values of 0.1, 0.2, 0.3, 0.4, 0.5 are compared. Frequency is varied from 0.2 Hz to 2 Hz with increments of 0.2 Hz.

For all computations, free-stream velocity is set to 0.1m/s and chord length of the airfoils is $c = 0.1$m. A virtual drag law is applied on airfoils to satisfy a steady state solution in an inviscid environment. For high Reynolds numbers, drag law is $D = \frac{1}{2} C_d S_w U^2$ where ρ is the density of the fluid, C_d is the coefficient of drag and S_w is the wetted surface area.

Results and Discussion

Figure 3 shows flow fields of 8 cycles of oscillations of a rigid and 5 different flexible airfoils. Trailing edge is passively deflecting, hence, fixing the Strouhal number to an exact value is not possible. Therefore within some tolerance, Strouhal number is set to $St = 0.5 \pm 0.04$. Actual downstream location of the vortex streets are shown without any scaling. Figure 3(a) shows the rigid case and flexibility of the airfoils increase going downwards in the figure. It is clear that at $St \approx 0.5$ rigid airfoil generates a deflected vortex street starting around 2 chord lengths downstream of the trailing edge. As flexibility increases, deflected jet first shifted back 5 chord lengths downstream in Figure 3(b) and vortex street becomes symmetric, Figure 3(c). Unlike the computational work conducted by Zhu et. al. (2014), further increasing the flexibility in our simulations did not trigger any symmetry breaking of the wake (see Figure (d), (e), (f)). Our model does not take the leading edge separation into consideration and even operating at structural resonance frequency, we observed a maximum angle of attack of 23°. Zhu et. al. modeled the leading edge separation in their study and their passive pitching amplitude went up as high as 50°. The separated flow from the leading edge interacts with the strong vortices shed from the trailing edge and leads to a deflected jet even for flexible cases.

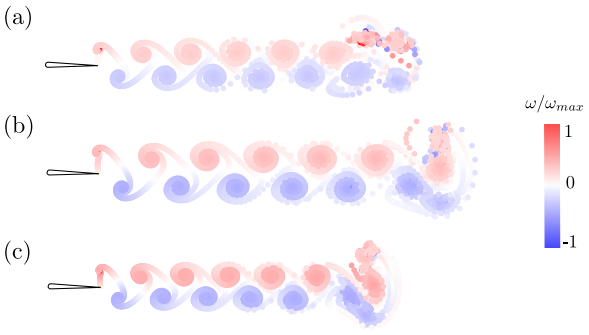

Figure 4: The flow fields of non-dimensional flexibilities of $\Pi = 0.2$ (a), $\Pi = 0.3$ (b), $\Pi = 0.4$ (c) at $St \approx 1.2$. The red and blue vortices represents the counter clockwise and clockwise vorticity, respectively.

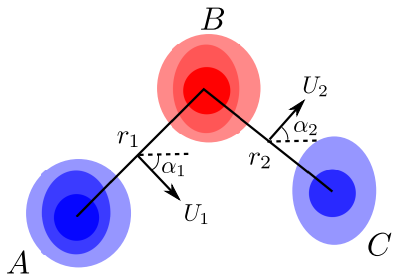

Figure 5: Schematic representation of two consecutive dipoles, A-B and B-C, together with the related parameters to calculate the induced velocities, U_1 and U_2.

A symmetry breaking threshold Strouhal number of around 0.4 is reported in the literature for rigid airfoils. Figure 4 represents the flow fields of 3 different flexible foils pitching with a $St = 1.17 \pm 0.01$. Although vortices are spaced very closely, the symmetry of the vortex street is preserved. It is clear that adding flexibility to the system makes Strouhal number an irrelevant parameter to determine the symmetry breaking phenomenon. To study the deflection characteristic of the wake, a dipole model can be used which was initially proposed by Zheng and Wei (2012). A schematic representation two consecutive dipoles are shown in Figure 5. Vortex A and vortex C induce velocities of U_1 and U_2 on vortex B with angles of α_1 and α_2, respectively. The magnitude of the induced velocities

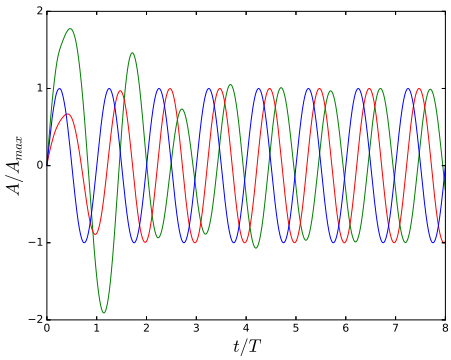

Figure 6: The trailing edge amplitudes normalized by the maximum amplitude of a rigid, blue, and 2 different flexible airfoils, red $\Pi = 0.3$, green $\Pi = 0.5$ as a function of 8 pitching cycles.

are determined by the Biot-Savart law as;

$$U = \frac{\Gamma}{2\pi r} \tag{9}$$

where Γ is the vortex circulation and r is the distance in between two vortices. In a symmetric vortex street the lateral components of U_1 and U_2 cancel each other out leaving the only induced velocity on vortex B in the horizontal direction. However, if the symmetry of the street is disturbed, the lateral velocity induced on vortex B becomes non-zero and deflection occurs.

The dipole model can be used to explain the flow fields observed in the current study. The trailing edge amplitudes normalized by the maximum amplitude across 8 flapping cycles is shown for one rigid and 2 flexible airfoils in Figure 6. For the flexible airfoils, a phase delay happens in between the input motion and the trailing edge motion in the first cycle. Consequently, although the vortices shed in the first cycle, together with the starting vortex, induce velocities with lateral components on the newly shed vortices, they convect further away downstream which in turn decreases their induced effect on the newly shed vortices. This mechanism prevents the jet inclination for the flexible airfoils. However, for the rigid case the motion is prescribed and there is no extra time for the first shed vortices to convect downstream. Additionally it can be observed that as flexibility increases, phase delay also increases. Thus, a large enough flexibility will create a long enough phase delay for attenuation of the induced velocity of the existing wake on the newly shed vortices.

Conclusion

In conclusion, consistent with the previous literature, we observed that introducing a flexibility model to a rigid airfoil inhibits the symmetry breaking phenomenon even for Strouhal numbers as high as 1.2. The jet deflection dependence on Strouhal number vanishes for flexible systems. A dipole model better explains the symmetry-asymmetry characteristics of the wake. Together with the dipole model, the amount of phase delay in the first flapping cycle turns out to be the critical parameter which determines the wake symmetry.

This study does not model leading edge separation. However, the maximum pitching angle is limited to 23°. For pure pitching motion, especially for high Strouhal numbers, the leading edge vortices would be weak and we do not believe that the observed flow field results would change dramatically.

Acknowledgements

This work was supported by the Office of Naval Research under Program Director Dr R. Brizzolara, MURI grant number N00014-14-1-0533.

References

[1] Dai, H., Luo, H., de Sousa, P. J. F., Doyle, J. F. (2012). Thrust performance of a flexible low-aspect-ratio pitching plate. Physics of Fluids (1994-present), 24(10), 101903.

[2] von Ellenrieder, Karl D., and Stamatios Pothos. "PIV measurements of the asymmetric wake of a two dimensional heaving hydrofoil." Experiments in fluids 44.5 (2008): 733-745.

[3] Emblemsvag, Jo-Einar, Ryuta Suzuki, and Graham Candler. "Numerical simulation of flapping micro air vehicles." AIAA Paper 3197 (2002).

[4] Godoy-Diana, Ramiro, Jean-Luc Aider, and Jos Eduardo Wesfreid. "Transitions in the wake of a flapping foil." Physical Review E 77.1 (2008): 016308.

[5] Godoy-Diana, Ramiro, et al. "A model for the symmetry breaking of the reverse Bnardvon Krmn vortex street produced by a flapping foil." Journal of Fluid Mechanics 622 (2009): 23-32.

[6] Jones, K. D., C. M. Dohring, and M. F. Platzer. "Experimental and computational investigation of the Knoller-Betz effect." AIAA journal 36.7 (1998): 1240-1246.

[7] Katz, J., Plotkin, A. (2001). Low-speed aerodynamics (Vol. 13). Cambridge University Press.

[8] Krasny, R. (1986). A study of singularity formation in a vortex sheet by the point-vortex approximation. Journal of Fluid Mechanics, 167, 65-93.

[9]Marais, C., Thiria, B., Wesfreid, J. E., Godoy-Diana, R. (2012). Stabilizing effect of flexibility in the wake of a flapping foil. Journal of Fluid Mechanics, 710, 659-669.

[10] Moore, M. Nicholas J. "Analytical results on the role of flexibility in flapping propulsion." Journal of Fluid Mechanics 757 (2014): 599-612.

[11] Ramananarivo, S., Godoy-Diana, R., Thiria, B. (2011). Rather than resonance, flapping wing flyers may play on aerodynamics to improve performance. Proceedings of the National Academy of Sciences, 108(15), 5964-5969.

[12] Shyy, W., Aono, H., Chimakurthi, S. K., Trizila, P., Kang, C. K., Cesnik, C. E., Liu, H. (2010). Recent progress in flapping wing aerodynamics and aeroelasticity. Progress in Aerospace Sciences, 46(7), 284-327.

[13] Zheng, Zhongquan Charlie, and Z. Wei. "Study of mechanisms and factors that influence the formation of vortical wake of a heaving airfoil." Physics of Fluids (1994-present) 24.10 (2012): 103601.

[14] Zhu, Xiaojue, Guowei He, and Xing Zhang. "How flexibility affects the wake symmetry properties of a self-propelled plunging foil." Journal of Fluid Mechanics 751 (2014): 164-183.